Open access • Journal Article • DOI:10.1680/ENER.11.00003

# Laterally loaded monopile design for offshore wind farms — Source link

Paul Doherty, Kenneth Gavin

**Published on:** 01 Feb 2012

**Topics:** Offshore wind power, Wind power, Offshore geotechnical engineering and Foundation (engineering)

| | |
|---|---|
| ***Title*** | Laterally loaded monopile design for offshore wind farms |
| ***Authors(s)*** | Doherty, Paul; Gavin, Kenneth |
| ***Publication date*** | 2011-12 |
| ***Publication information*** | Proceedings of the ICE - Energy, 165 (1): 7-17 |
| ***Publisher*** | Institution of Civil Engineers |
| ***Item record/more information*** | http://hdl.handle.net/10197/4073 |
| ***Publisher's statement*** | Permission is granted by ICE Publishing to print one copy for personal use. Any other use of these PDF files is subject to reprint fees. |
| ***Publisher's version (DOI)*** | 10.1680/ener.11.00003 |

**Energy**
Volume 165 Issue EN1

**Laterally loaded monopile design for offshore wind farms**
Doherty and Gavin

ice | proceedings

**Proceedings of the Institution of Civil Engineers**
Energy 165 February 2012 Issue EN1
Pages 7–17 http://dx.doi.org/10.1680/ener.11.00003
**Paper 1100003**
Received 06/01/2011 Accepted 28/04/2011
Published online 19/12/2011
**Keywords:** codes of practice & standards/offshore engineering/renewable energy



ice
Institution of Civil Engineers
publishing

# Laterally loaded monopile design for offshore wind farms

**Paul Doherty** BE, PhD
Post-Doctoral Researcher, Geotechnical Research Group, School of Architecture, Landscape and Civil Engineering, University College Dublin, Dublin, Ireland

**Kenneth Gavin** BEng, PhD
Geotechnical Lecturer, Geotechnical Research Group, School of Architecture, Landscape and Civil Engineering, University College Dublin, Dublin, Ireland

**Expansion of the offshore UK wind energy sector has stimulated renewed interest in the response of piles to lateral and moment loads. This paper compares the state of the art in foundation design with current industry trends in offshore wind turbine construction. The historical evolution of pile design for lateral loading is described in detail, focusing on the American Petroleum Institute guidelines used by the offshore sector. The limitations of these design codes are discussed in light of the specific requirements for the wind sector. Recent research efforts attempting to bridge the gap between practice and industry are highlighted and further research needs are identified.**

## Notation

| | |
|---|---|
| $A$ | empirical lateral resistance factor |
| $B$ | empirical lateral resistance factor |
| $C_1$ | dimensionless API coefficient |
| $C_2$ | dimensionless API coefficient |
| $C_3$ | dimensionless API coefficient |
| $D$ | pile diameter |
| $E_\mathrm{p}$ | pile Young's modulus |
| $E_{py}$ | secant spring stiffness |
| $E_{py}^0$ | initial secant spring stiffness |
| $E_\mathrm{s}$ | soil Young's modulus |
| $I_\mathrm{p}$ | moment of inertia |
| $K_0$ | in situ earth pressure coefficient |
| $k$ | initial modulus of subgrade reaction |
| $L$ | embedded pile length |
| $p$ | soil reaction |
| $p_\mathrm{c}$ | theoretical ultimate resistance |
| $p_\mathrm{m}$ | measured resistance |
| $p_\mathrm{u}$ | ultimate resistance |
| $R$ | pile rigidity factor |
| $x$ | depth |
| $y$ | lateral deflection |
| $\gamma$ | unit weight of soil |

## 1. Introduction

Increasing political and societal pressures to reduce carbon dioxide emissions and society's dependence on fossil fuels have driven the demand for green sustainable energy sources. As a result, the UK's offshore wind sector has undergone rapid and continuous growth over the past decade. This growth is driven by ambitious targets to achieve up to 35% of electricity generation from renewable sources by 2020 and is thus set to continue for the next decade. Onshore wind has been successfully harnessed in many countries. However, the land requirements and aesthetics of onshore turbines are often considered undesirable. Offshore wind farms have a number of clear advantages, namely

(*a*) their limited aesthetic impact by locating them far from land
(*b*) high unrestricted wind speeds, which are generally more consistent than onshore
(*c*) higher power generation through the use of large-capacity turbines.

In order to realise the proposed energy targets, the Crown Estate, which controls the UK seabed, has awarded 'round 3' development licences for nine offshore sites that will ultimately produce 35 GW of electricity by 2020.

As the round 3 projects will be completed in deeper waters (>30 m) and turbines with higher capacities are becoming available, future wind turbines will be subjected to high lateral and moment loads. These turbines will require robust foundations with adequate stiffness to prevent unacceptable displacements or rotations of the structure.

Considering these issues, this paper presents an overview of the current offshore pile design standards for lateral loading. The historical evolution of existing pile design approaches is described. The limitations of current methods, which were originally developed for the oil and gas industry, are discussed in light of the loading conditions and pile geometries commonly encountered in the offshore wind sector. The discussion is limited to sandy soils because of their widespread prevalence around the UK coast and in the North Sea. Recent experimental and numerical advances are highlighted and areas requiring further research are identified.

## 2. Foundation design issues for offshore wind

The first offshore wind farm was installed off the Danish coast in 1991 and was supported on a gravity base, similar to those used for the majority of onshore wind turbine foundations. However, a number of other substructure options have subsequently been used offshore, including monopiles, jackets/tripods and, more recently, floating turbines tethered to the seabed with tension anchors. These foundation concepts are illustrated schematically in Figure 1. In shallow water, and where the ground conditions below the seabed have adequate bearing capacity, concrete gravity bases have proved successful. Gravity foundations resist the applied load through the bearing resistance of the underlying soil strata and the dead weight of the concrete base. In suitable ground conditions, monopiles (comprising a single large-diameter steel tube driven into the seabed) have proven to be an efficient solution in water depths up to 35 m. These piles resist lateral wind and wave loading (and resulting moments) by mobilising horizontal earth pressures in competent near-surface soils. In water depths ranging from 35 to 60 m, jacket structures have been used to support wind turbines. The jacket consists of a three- or four-legged steel lattice frame founded on single piles placed below each leg. The applied loads are transferred through the jacket structure into the foundation piles, where resistance is generated through axial push–pull action. As a result, the tension pile capacity often governs the design process for jacket piles. A recent pilot project off the coast of Norway has demonstrated the possibility of using deep-water floating turbines. However, the commercial viability of floating designs remains uncertain.

The geographical distribution of offshore wind farms constructed around the UK is illustrated in Figure 2. Monopiles are by far the most common support structure, accounting for over 75% of existing turbine foundations, as shown in Figure 3. To date, monopiles have been the most economic alternative due to their competitive fabrication and installation costs coupled with the relatively shallow-water depths at existing sites. However, the majority of sites planned for development over the next 10–15 years are located in water depths ranging from 30 to 70 m and, as a result, are largely outside the scope of existing installation experience. This is a specific and significant concern for many of the round 3 development sites, which are also illustrated in Figure 2.

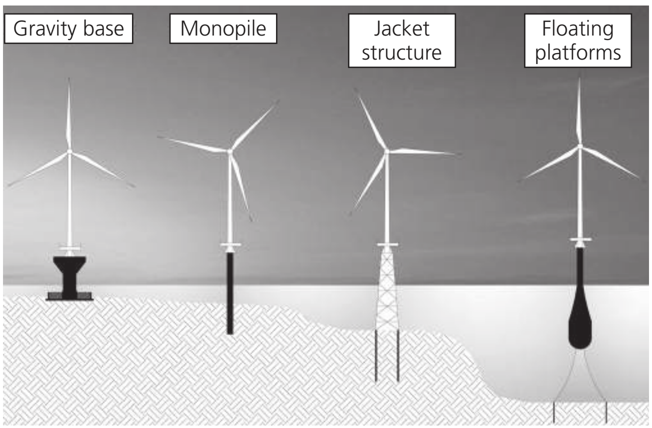


Figure 1. Foundation concepts for offshore wind turbines

The average water depths for wind farms that are currently in the design phase are compared with those currently in operation in Figure 4. The transition to deeper water, evident in the figure, will result in the span between the turbine superstructure and the seabed also increasing. This, coupled with more extreme environmental loading from higher magnitude wind and waves, results in larger moments applied to the foundation. While monopiles are an attractive solution for developers and designers alike, the increased water depths would result in larger diameters with stiffer cross-sections. The monopiles used to date consist of a stiff pile of diameter 4–6 m and penetration depths ranging from 20 to 30 m. This results in slenderness ratios of approximately 5–6. The design of these foundation elements is normally performed using semi-empirical formulas developed for the offshore oil/gas industry from field tests on significantly smaller diameter piles. Extrapolating these methods to the geometries considered today requires careful consideration of the applied loading and the inherent limitations underlying the current design methods.

Typical loading conditions for an offshore monopile are illustrated schematically in Figure 5. The loads are shown to be acting at the interface level between the monopile and the turbine shaft. An axial load of approximately 6 MN and a lateral load of 2 MN act at this point. In addition, a high moment is generated by the turbine lever arm, which combines lateral wind forces with the rotor height above the interface level. The water depth will generate a further moment load on the monopile at the seabed level (resulting from the 2 MN lateral component). It is clear from Figure 5 that monopile design is controlled by the lateral and moment loads and efficient foundations can therefore only be achieved by addressing uncertainties in the lateral loading design processes.

## 3. Evolution of current design standards

The most popular method of analysis for laterally loaded piles, and the method adopted in the offshore design codes of the American Petroleum Institute (API, 2007) and Det Norske Veritas (DNV, 2007), is based on the Winkler model and is commonly referred to as the *p–y* approach. This method of analysis assumes that the pile acts as a beam supported by a series of uncoupled springs, which represent the soil reaction. These springs, illustrated in Figure 6, can be characterised by a

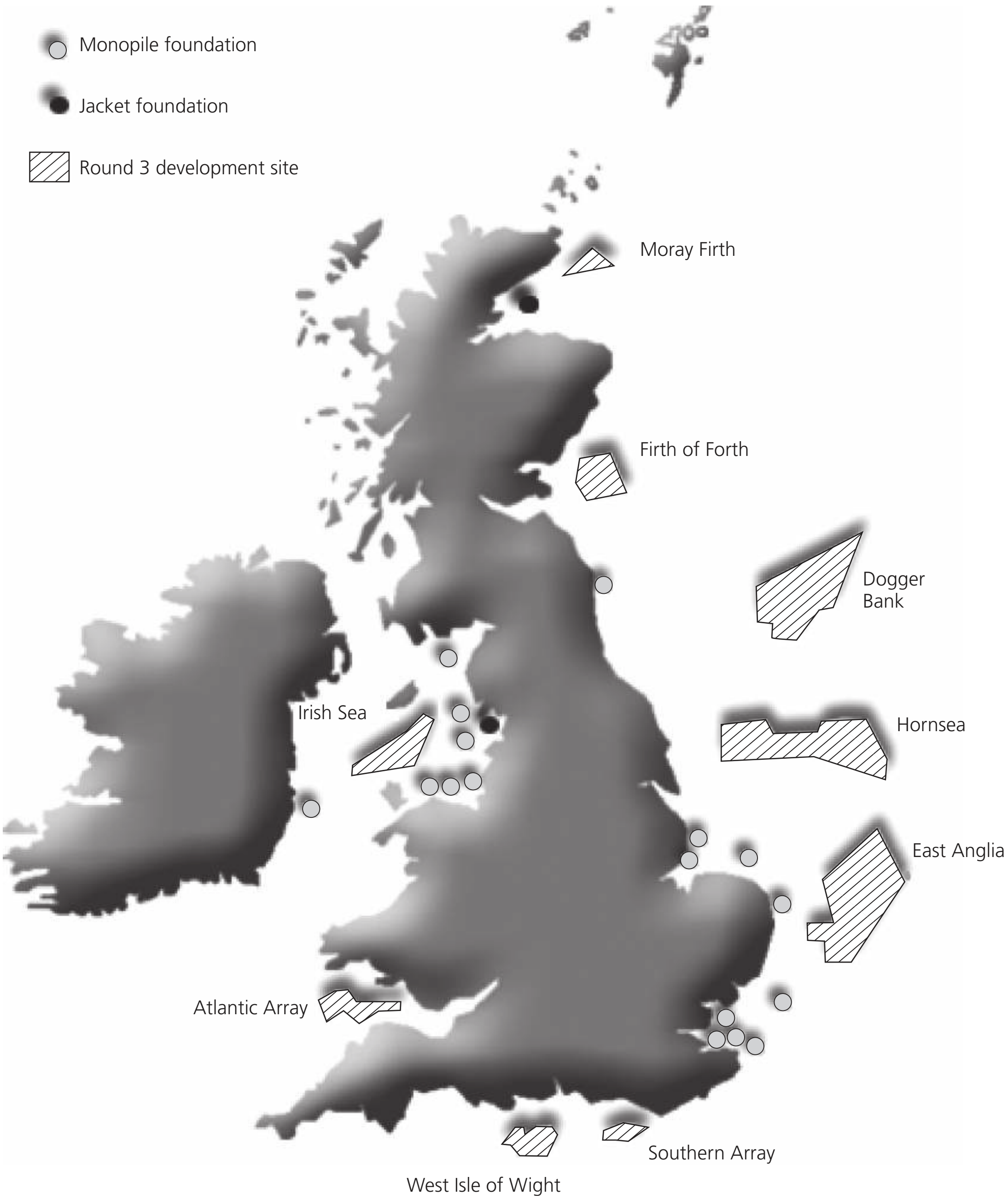


**Figure 2.** Locations of UK's existing offshore wind farms and round 3 development sites

linear or non-linear curve, which describes the soil reaction $p$ at a given depth as a function of the lateral movement $y$. The spring stiffness $E_{py}$ is defined as the secant modulus of the $p$–$y$ curve (see Figure 6).

The Winkler approach was first introduced in 1867, with Hetenyi (1946) providing a solution to the problem of a beam on an elastic foundation. Following on from this, the $p$–$y$ concept was originally suggested by Reese and Matlock in 1956. Subsequent experimental research conducted by Matlock (1970) demonstrated that the soil resistance at a given point on the pile is independent of the pile deflections at points above and below that point, supporting the underlying assumption that the springs are uncoupled in the $p$–$y$ approach. The original $p$–$y$ curves for piles in cohesionless deposits were developed by Reese *et al.* (1974) and were empirically derived from the results of lateral load tests on two identical instrumented test piles at Mustang Island in Texas described by Cox *et al.* (1974).

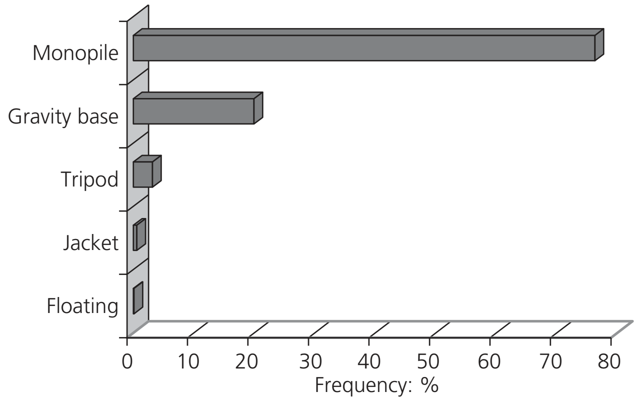


**Figure 3.** Foundation distribution for offshore wind turbines

The Mustang Island tests were performed on steel tubes of diameter $D = 610$ mm, with a wall thickness of 9·5 mm, driven open-ended to a penetration depth $L$ of 21 m into saturated sand and laterally loaded with a free-ended boundary condition. The corresponding $L/D$ ratio of 34 for these piles is significantly larger than the slenderness ratios typical of the wind industry ($L/D = 5$–6). The soil properties at the test site were estimated from the results of standard penetration tests (SPTs) conducted in two boreholes adjacent to the test pile locations. The strength parameters were subsequently determined from correlations by Peck *et al.* (1953). The soil conditions at the site were highly variable, with SPT $N$ values ranging from 10 to 80 over the upper 12 m. The piles were loaded both statically and cyclically. Strain gauges, placed at 34 locations along the pile shaft, measured the bending moment profile with depth. Integration and differentiation of the bending moment profile allowed Reese *et al.* (1974) to determine the experimental $p$–$y$ curves. These curves were combined with some theoretical predictions based on lateral soil–pile failure modes for shallow- and deep-soil behaviour. The combined analysis resulted in semi-empirical $p$–$y$ curves that consisted of four discrete parts assembled into a continuous piecewise curve (see Figure 7). The initial portion of the curve is a straight line, which is

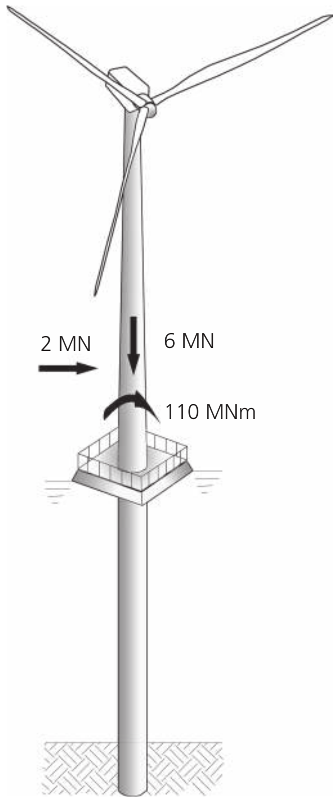


**Figure 5.** Monopile loading schematic

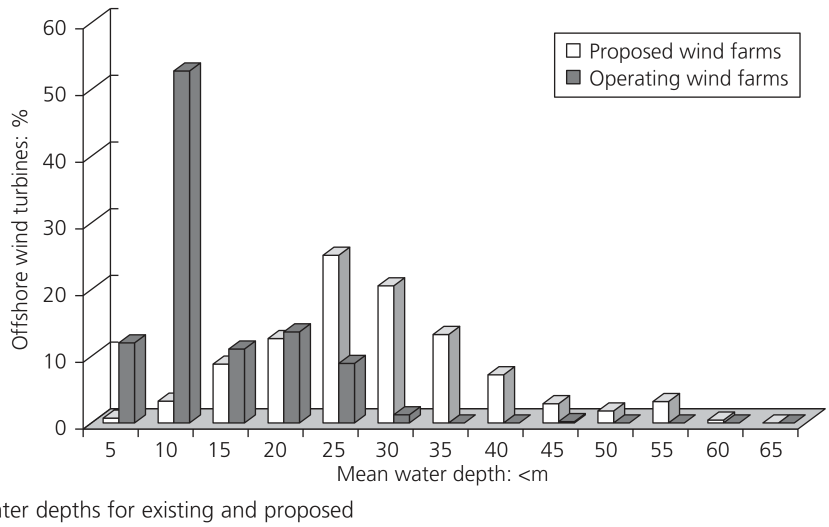


**Figure 4.** Variation in water depths for existing and proposed wind farms

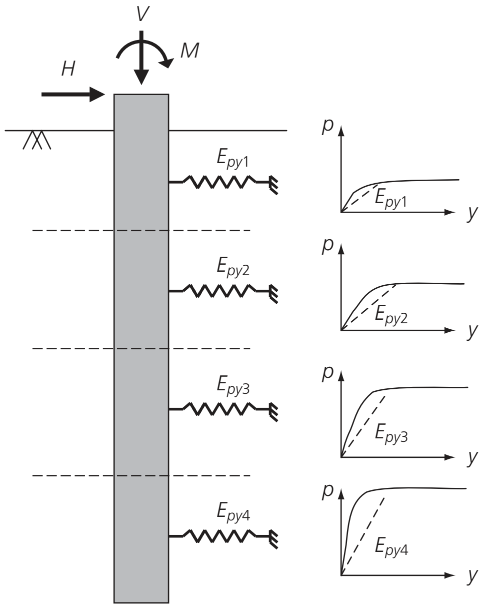


**Figure 6.** Winkler *p–y* model for lateral loading

followed by a parabola adjoined to another linear portion and finally a constant ultimate strength, with each portion of the curve derived as follows.

(*a*) The theoretical ultimate resistance $p_c$ was derived by assuming that, at shallow depths, an active Rankine-type wedge failure developed in front of the pile and a passive wedge acted behind the pile, with the active force determined from the minimum coefficient of earth pressure. At deeper levels, a block-type shear failure was assumed with the sand flowing around the pile. The transition depth between these modes of failure is determined where the soil resistances given by the two modes of failure are equal. For piles with low slenderness ratios (as is typically the case for monopiles), the shallow failure mechanism can act over the entire pile shaft. Despite the theoretical nature of this approach, it resulted in poor predictions of the ultimate resistance for the Mustang Island tests and, as a result, $p_c$ had to be multiplied by a depth-dependent empirical factor $A$ (Figure 8(a)). The ultimate resistance $p_u$ was deemed fully mobilised at a deformation of $3D/80$, as illustrated in Figure 7, with a perfectly plastic condition assumed for larger displacements.

(*b*) An additional empirical parameter $B$ (Figure 8(b)) was used to fit $p_c$ with the measured resistance $p_m$ at a deformation of $D/60$. A linear increase in resistance was assumed between $p_m$ and $p_u$.

(*c*) The initial portion of the curve was obtained using a linear resistance relationship, where $p = E^0_{py}y$. The initial stiffness $E^0_{py}$ increases linearly with depth $x$ ($E^0_{py} = kx$). The increase is defined by the initial modulus of subgrade reaction $k$, which depends on the relative density, with Reese *et al.* (1974) suggesting values of 5·4, 16·3 and 34 $MN/m^3$ for loose, medium and dense sands respectively.

(*d*) The intermediary section of the original *p–y* curve was described by a parabola that adjoins the straight line portions of the curves, as illustrated in Figure 7.

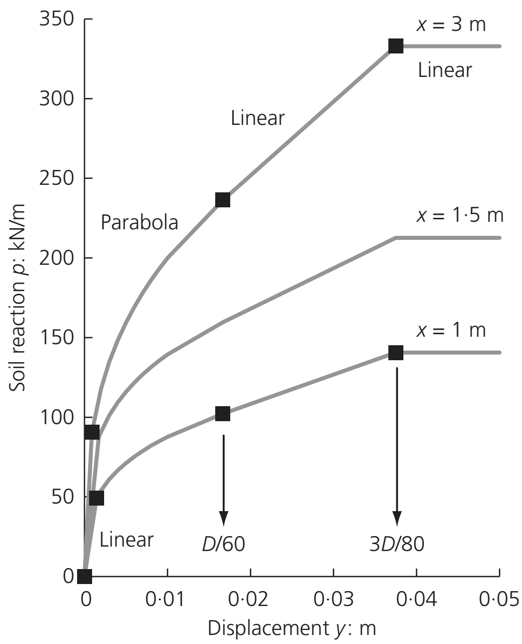


**Figure 7.** Example *p–y* curves generated by the Reese *et al.* (1974) approach

The load tests reported by Reese *et al.* (1974) at Mustang Island included a series of cyclic tests that were used to develop *p–y*

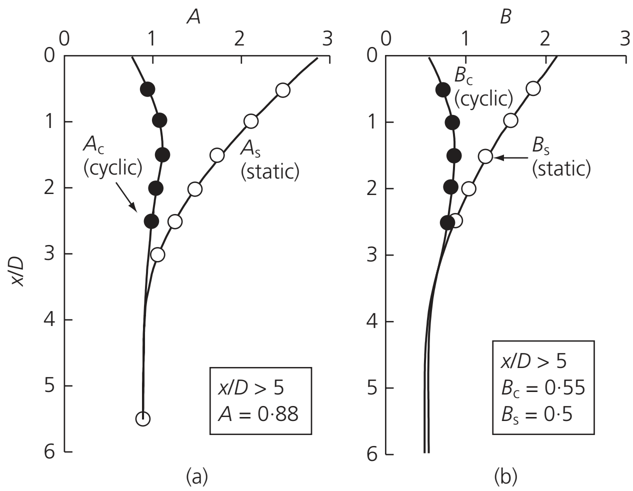


**Figure 8.** Empirical parameters proposed by Reese *et al.* (1974)

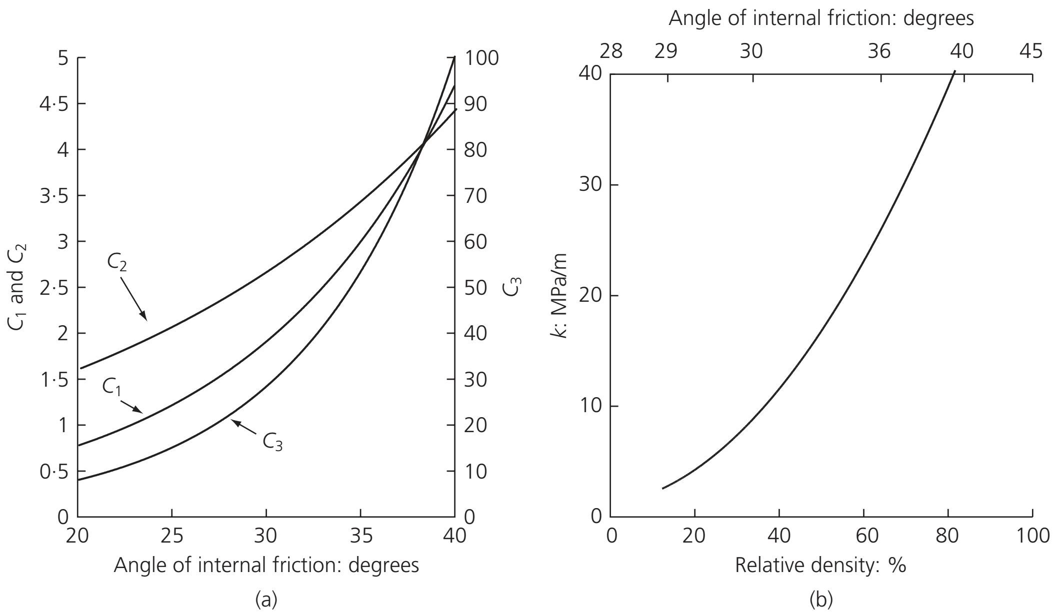


**Figure 9.** (a) $C$ coefficients and (b) initial modulus of subgrade reaction $k$ for API RP2A (API, 2007)

curves that captured the pile–soil cyclic response. The mobilised resistance of the piles reduced during cyclic loading and the two empirical factors $A$ and $B$ were introduced to account for this degradation (see Figure 8). This type of analysis gives an ultimate value for the $p$–$y$ curves or a degraded curve. However, it does not consider the transitional period between the static and ultimate cyclic curve and thus does not provide a method of considering the pile rotations or accumulated displacements during cycling.

A research study sponsored by the API compiled a pile test database and tested the accuracy of the Reese *et al*. (1974) model against three alternative $p$–$y$ formulas (Murchinson and O'Neill, 1984). A hyperbolic model, given by Equation 1, was shown to provide better predictions of the lateral deflections and the maximum moments than the traditional 1974 approach and this model has been incorporated into current design methods (API, 2007; DNV, 2007). The ultimate resistance for this model is determined using the same methodology (based on Rankine earth pressures) as previously established. However, estimating $p_u$ is simplified by introducing the dimensionless coefficients $C_1$, $C_2$ and $C_3$, which are functions of the friction angle (see Figure 9(a)). The ultimate soil resistance can then be determined without the need to calculate the Rankine pressures acting on the pile by using Equation 2.

1. $$p = Ap_\mathrm{u}\tanh\left(\frac{kx}{Ap_\mathrm{u}}y\right)$$

2a. $$p_\mathrm{u} = \min\left(p_\mathrm{us}, p_\mathrm{ud}\right)$$

2b. $$p_\mathrm{us} = (C_1x + C_2D)\gamma x$$

2c. $$p_\mathrm{ud} = C_3D\gamma x$$

3. $$A = \left(3 - 0.8\frac{x}{D}\right) \geqslant 0.9$$

The $p$–$y$ curve given by Equation 1 incorporates the previously described empirical parameter $A$, which can be calculated from Equation 3 for static loading or selected directly from Figure 8(a). For cyclic loading $A = 0{\cdot}9$ should be used. By directly including this parameter to determine the soil reaction at failure, API RP2A (API, 2007) is directly calibrated against the load tests conducted at Mustang Island on flexible piles. The pile–soil stiffness can be obtained by differentiating Equation 1

4. $$E_{py} = \frac{\mathrm{d}}{\mathrm{d}y}\left[Ap_\mathrm{u}\tanh\left(\frac{kx}{Ap_\mathrm{u}}y\right)\right] = Ap_\mathrm{u}\frac{kx/Ap_\mathrm{u}}{\cosh^2(kxy/Ap_\mathrm{u})}$$

Following Equation 4, the initial stiffness at a displacement of zero gives $E_{py}^0 = kx$, which agrees with the originally adopted assumption of linearly increasing stiffness with depth. The discrete values of $k$ proposed by Reese *et al*. (1974) were replaced in the current API design code API RP2A (API, 2007) by the curve shown in Figure 9(b) to allow an appropriate $k$ value to be determined for a range of relative densities/friction angles. However, this curve only shows values of $k$ up to 80% relative density, which introduces considerable errors in the estimation of $k$ for very dense deposits, as commonly found in the North Sea.

The Murchinson and O'Neill (1984) database consisted of 14 load tests on piles with diameters up to 1·22 m installed in loose to dense sand. However, the final conclusion of the study was that

> The database was small ... Further high quality field tests, especially on instrumented, large diameter piles, are needed to enlarge the database and to permit future reassessment of procedures for analysing laterally loaded piles in cohesionless soils.

Unfortunately, 25 years later and the API code has largely remained unchanged, despite the obvious limitations of the original formulations and the specific needs of the newly emerged wind energy sector.

## 4. Limitations of existing standards

The current API/DNV methods are a slightly modified version of the original *p–y* method proposed by Reese *et al.* (1974) but the underlying principals and methodology remain the same. The empirical basis of this method reduces confidence in extrapolating this method beyond the original formation dataset, which consisted of two 610 mm diameter flexible piles and a slightly larger test database by Murchinson and O'Neill with piles up to 1·22 m in diameter. However, there remains no lateral test data for piles in the range 4–6 m diameter, where these design methods are currently being applied. This empiricism underpins the major limitations of API RP2A (API, 2007).

### 4.1 Mode of failure

A number of researchers have postulated that the pile response and failure mechanism depends on the flexibility of the pile itself (e.g. Briaud *et al.*, 1984; Budhu and Davies, 1987; Dobry *et al.*, 1982). Poulos and Hull (1989) used the rigidity parameter $R$, dependent on the pile Young's modulus $E_p$, moment of inertia of the pile $I_p$ and soil stiffness $E_s$, to classify the pile response

$$R = \left(\frac{E_p I_p}{E_s}\right)^{0.25} \quad (5)$$

Poulos and Hull suggested that a pile behaves rigidly if the length is less than 1·48$R$ and behaves flexibly if the length exceeds 4·44$R$. The length normalised by the rigidity parameter ($L/R$) is plotted as a function of slenderness ratio ($L/D$) in Figure 10 for piles with a wall thickness of 50 mm. For typical monopile geometries, with slenderness ratios in the range 4–6, piles installed in loose sand are very likely to exhibit rigid failure according to the relationships proposed by Poulos and Hull (1989). For very stiff sand with an $E_s$ value of 100 MPa, the failure mechanism is less certain, with typical monopile geometries falling in the transition range between rigid and flexible behaviour. For most monopile installations the soil stiffness will be significantly less than 100 MPa and a

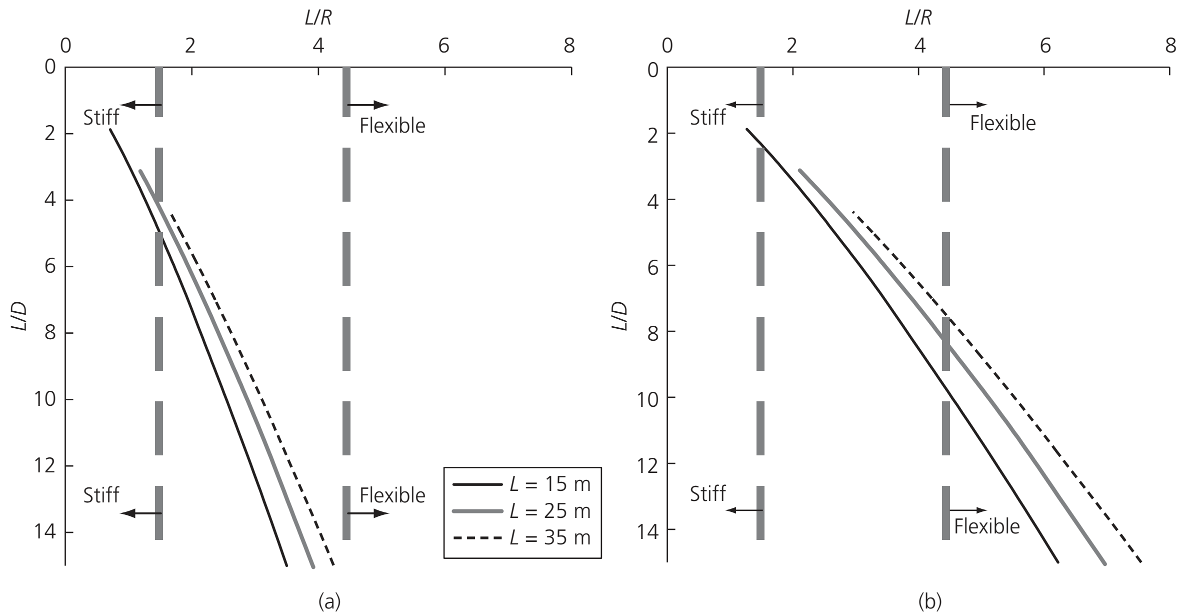


**Figure 10.** Pile failure mechanism for soils with (a) $E_s = 10$ MPa and (b) $E_s = 100$ MPa

rigid failure mechanism will occur. This rigid failure mechanism is supported by observations from model tests of monopiles installed in dense sand subjected to lateral loads (e.g. Leblanc *et al.*, 2010).

The rigid mode of failure casts considerable doubts on the validity of applying the existing *p–y* curves (which were developed to match the response of flexible piles) to predict the behaviour of offshore monopiles. API RP2A needs to be urgently calibrated for rigid pile behaviour to determine the initial stiffness and ultimate capacity.

API RP2A also assumes the pile to exhibit a Rankine-type failure in determining $p_u$. This assumes that a frictionless interface exists between the pile and the soil (or that the pile is perfectly smooth), whereas in reality the pile will exhibit friction as the sand flows around the pile shaft. Briaud *et al.* (1984) proposed a model to consider both the frontal and shear components of resistance; there are, however, limited experimental results with which to calibrate the model and the shear resistance has not been incorporated into API RP2A. Another component of resistance that is neglected in the current approach is the shear resistance mobilised at the pile base and the shear resistance mobilised between adjacent soil layers (which is discounted by the assumption of independent decoupled springs). As the pile fails rigidly, the soil will also mobilise a passive wedge beneath the point of zero deflection, which is not considered in the current methodology. The accumulated errors from ignoring these components of resistance are possibly partially offset by incorporating the empirical coefficient $A$. However, it remains uncertain whether these components of resistance, combined with the rigid failure mechanism, are accurately accounted for when API RP2A is extrapolated to large-diameter piles.

### 4.2 Impact of diameter

According to API RP2A (API, 2007), the initial modulus of subgrade reaction is only dependent on the sand relative density and is independent of diameter – a point worthy of question and one that has received considerable attention in the literature.

Terzaghi (1955) examined the impact of geometry on the stress bulbs mobilised during failure of the soil and concluded that as the pile diameter increased the mobilised stress bulb increased in size. This effect results in a greater displacement under the same soil pressure. However, the soil pressure acting at the pile shaft reduces as the pile diameter increases and, as a result, the modulus of subgrade reaction $E_{py}$ is independent of the pile diameter. Vesic (1961) used elasticity theory to propose a modulus of subgrade reaction that was based on both pile and soil properties. This relationship was shown to be relatively independent of the diameter. In contrast, Pender (1993) showed that the initial stiffness was linearly dependent on the pile diameter by using a simple hyperbolic soil model. These studies concerned the modulus of subgrade reaction $E_{py}$. However, the results can be considered applicable to the initial modulus $E_{py}^0$ or the stiffness parameter $k$.

The contrasting findings of previous researchers prompted Ashford and Juirnarongrit (2005) to conduct a dedicated study into diameter effects. They employed a simple finite-element model (FEM) and varied the pile diameter while maintaining a constant bending stiffness. The analysis showed that increasing the diameter had a positive influence on the pile response, reducing both the displacements and the depth to the maximum moment. However, the research concluded that the effect of increasing the diameter was relatively small in comparison with the impact of the pile bending stiffness. The FEM results were supported by back-analysis of *p–y* curves from static load tests, which showed a negligible impact of pile diameter. Further analysis by Ashford and Juirnarongrit (2005) involved measuring the accelerations of bored piles subjected to small lateral vibrations and comparing the in situ frequencies with those determined from a numerical model with an assumed soil modulus. Pile diameters of 0·6, 0·9 and 1·2 m were used in the study and the best match between the measured results and the predicted behaviour was obtained when a soil modulus independent of diameter was used. They concluded that there was no significant relationship between $E_{py}$ and the pile diameter, supporting the findings of Vesic (1961) and Terzaghi (1955). Fan and Long (2005) also conducted an FEM investigation in which the pile diameter was increased while maintaining a constant bending stiffness, $E_pI_p$. This research concluded that there was no significant correlation between pile diameter and initial stiffness. However, the analysis considered traditional slender piles.

Lesny and Wiemann (2006) conducted FEM analyses and showed the initial stiffness of the *p–y* curves developed along the shaft of a monopile varied according to a power law with depth, such that at significant depths the stiffness was overestimated by the traditional *p–y* curves and hence the API method was unconservative for large-diameter piles. They concluded that this could result in the current design methods predicting insufficient and unsafe pile embedment lengths. Sørensen *et al.* (2009) reported 3D Flac analyses and laboratory-scale lateral load tests that confirmed these findings. However, Sørensen *et al.* also determined that the initial stiffness of the *p–y* curves increased with pile diameter but was independent of both the pile bending stiffness and embedded length.

Lam (2009) used concepts developed for drilled shaft foundations supporting electricity transmission pylons to explain the apparent increase in stiffness and resistance with increasing pile diameters. Lam suggested that piles with a free-headed condition (like monopiles) developed additional resistance during lateral loading from the rotation of the pile shaft. Implementing moment–rotation springs parallel to lateral *p–y* springs resulted in a diameter-dependent model that showed improved predictions when compared with field tests reported by Lam and Martin (1986).

In light of the varied and contradictory evidence in the literature regarding diameter effects (and in particular regarding the impact on the initial *p–y* stiffness), there is considerable scope for further research to establish a more fundamental understanding of the scaling influence. The dearth of field tests on large-diameter piles is noticeable throughout the literature and makes validation of new theories and calibration of numerical models very difficult. This is particularly evident when comparing the database used by Murchinson and O'Neill (1984) to develop the existing API approach with the monopile diameters being installed today (see Figure 11). The need for further industrial-scale tests is an area that the wind industry needs to consider in order to validate the current design approaches for the geometries of current foundations.

### 4.3 Horizontal earth pressure coefficient

The horizontal earth pressure coefficient at rest $K_0$ is considered by Reese *et al.* (1974) to equal 0·4 and this constant value is incorporated into the calculation of the soil reaction at failure. The soil's relative density, friction angle and stress history has been shown by Mayne and Kulhawy (1982) to impact on the value of $K_0$, but this has not been considered in the current approach as the value is independent of the soil state. Fan and Long (2005) conducted finite-element analysis that considered the impact of varying $K_0$ on lateral monopile behaviour and determined that an increase in $K_0$ resulted in a significant increase in the ultimate soil resistance, as shown by the *p–y* curves at a depth of 2 m in Figure 12. The increase in ultimate soil resistance was also reflected in an increase in stiffness,

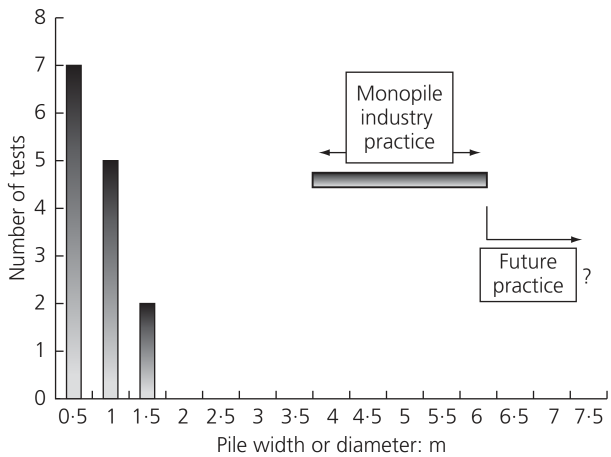


Figure 11. Comparison of the API database used by Murchinson and O'Neill (1984) with current practice and possible future practice

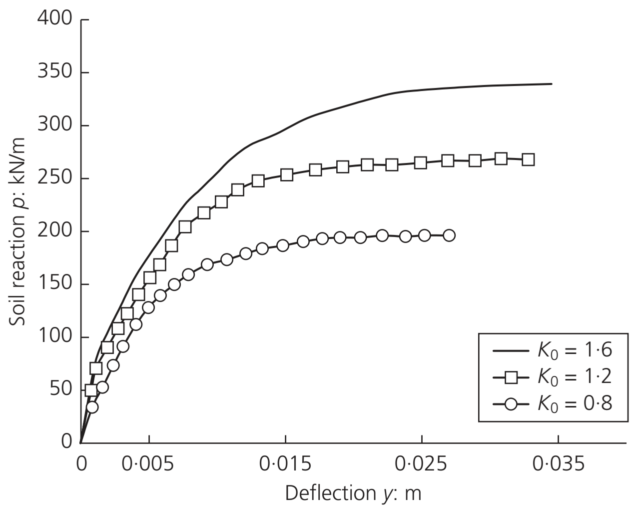


Figure 12. Impact of $K_0$ on the *p–y* curves (adapted from Fan and Long (2005))

with the parameter *k* mirroring the increase in $K_0$. This could have a dramatic impact on the response of piles installed in dense deposits that are likely to have high $K_0$ coefficients. Dense soils in the North Sea can exhibit very high cone tip resistance values of over 50 MPa at relatively shallow depths, suggesting very high in situ $K_0$ values. Following the findings of Fan and Long (2005), this would indicate that the API (2007) method would be excessively conservative in these conditions. However, the operational $K_0$ value will also be significantly affected by the installation method. The at-rest earth pressure adjacent to the pile after driving may be significantly lower than the in situ $K_0$ value due to friction fatigue effects developed as the pile is advanced into the ground (see Jardine *et al.* (2005) and Gavin *et al.* (2011)). This raises further concerns about the uncertainty of the operational $K_0$ value during lateral loading.

### 4.4 Impact of pile properties

Despite the *p–y* stiffness $E_{py}$ being a soil–structure interaction parameter, the existing codes only consider soil properties in formulating the *p–y* curves. Norris (1986) offered an alternative method of analysing the pile behaviour to lateral loading; known as the strain wedge (SW) model, it assumes a 3D wedge-type failure and considers pile stiffness directly in the *p–y* analysis. Ashour and Norris (2000) used the SW method to investigate the impact of pile properties on the mobilised *p–y* curve and found the stiffness and ultimate resistance increased dramatically as the piles' bending stiffness ($E_pI_p$) increased. By contrast, Fan and Long (2005) varied the Young's modulus of monopiles in an FEM analysis while maintaining the diameter and moment of inertia constant, and found no significant influence on the *p–y* curves. To date, there are insufficient experimental results to validate the conclusions of either Fan and Long (2005) or Ashour and Norris

(2000), and the influence of pile properties on the mobilised *p–y* curves remains an open question.

### 4.5 Cyclic loading considerations

Monopiles are typically designed to a strict serviceability tolerance, which is usually specified as a total rotation of less than 1°. The installation tolerance is usually 0·5° and therefore the deflection under in-service loading is usually designed not to exceed 0·5° rotation. Considering that the primary load components for wind turbine design are wind/wave/current and tidal loads, which all exhibit cyclic behaviour, the cyclic pile response is a major design consideration. However, the change in stiffness due to cyclic loading and accumulated displacements/rotation over time are not considered explicitly in the current codes as the cyclic *p–y* curves only consider the ultimate degraded resistance available following cyclic loading. In addition, considerable differences of opinion exist throughout the literature on the rate of cyclic displacement accumulation. Leblanc *et al.* (2010) used small-scale laboratory tests on stiff piles to develop a model for predicting pile rotations in response to continuous cyclic loading. The model assumes accumulated pile rotation to develop as a power function of the number of cycles *N*, in agreement with the earlier work of Little and Briaud (1988) and Long and Vanneste (1994). By contrast, Lin and Liao (1999) suggested a logarithmic trend to capture the accumulated strains caused by variable-amplitude load cycling on a database of 20 field-scale piles. In addition, Lin and Liao (1999) describe the factors affecting the cyclic response, which included loading type, type of pile installation, soil properties, pile embedment length and pile/soil relative stiffness ratio. Considering this array of influencing factors, the empirical parameters describing the logarithmic change in pile rotation should be viewed cautiously. Another caveat of the Lin and Liao study was the limited number of cycles (<50), which complicates extrapolation to longer duration cyclic loading. Overall, there is no standard approach or consensus in the literature for calculating lateral pile response to cyclic loading.

## 5. Conclusions

Offshore wind farms are typically supported on large-diameter monopiles. The dimensions of these foundation elements are outside the scope of current experience and, as a result, the current design procedures for lateral loading (API, 2007) are being extrapolated well outside the original dataset, which largely consists of a single set of pile tests at a medium-density sand site. The empiricism of this approach results in a number of discrepancies, which require urgent research attention. The main limitations and differences between the 2007 API design code and industry practice are as follows.

(*a*) The mode of failure is considerably different.
(*b*) Components of resistance are neglected (side shear/base shear).
(*c*) Diameter effects are uncertain.
(*d*) The linear increase in stiffness with depth is questionable.
(*e*) The underlying earth pressure coefficient is unverified.
(*f*) Pile properties are ignored in the existing approach.
(*g*) Cyclic loading and accumulated rotations are poorly considered.

## Acknowledgements

The first author would like to acknowledge Mainstream Renewable Power, IRCSET, Enterprise Ireland and Science Foundation Ireland for financial awards which were gratefully received. I would also like to thank Dr David Igoe for providing valuable technical comments.

**REFERENCES**

API (American Petroleum Institute) (2007) API RP2A: Recommended practice for planning, designing and constructing fixed offshore platforms. Working stress design, 22nd edn. API, Washington, DC.

Ashford SA and Juirnarongrit T (2005) *Effect of Pile Diameter on the Modulus of Subgrade Reaction*. Department of Structural Engineering, University of California, San Diego, CA.

Ashour M and Norris G (2000) Modelling lateral soil–pile response based on soil–pile interaction. *ASCE Journal of Geotechnical and Geoenvironmental Engineering* **126(5)**: 420–428.

Briaud JL, Smith T and Meyer BJ (1984) ASTM STP 835: Laterally loaded piles and the pressuremeter. Laterally loaded deep foundations: analysis and performance. American Society for Testing and Materials, West Conshohocken, PA, pp. 97–111.

Budhu M and Davies T (1987) Nonlinear analysis of laterally loaded piles in cohesionless soils. *Canadian Geotechnical Journal* **24(2)**: 289–296.

Cox WR, Reese LC and Grubbs BR (1974) Field testing of laterally loaded piles in sand. *Proceedings of the 6th Annual Offshore Technology Conference*, *Houston*, *TX*, 459–472.

DNV (Det Norske Veritas) (2007) DNV-OS-J101: Design of offshore wind turbine structures. DNV, Oslo.

Dobry R, Vincente E, O'Rourke M and Roesset J (1982) Stiffness and damping of single piles. *Journal of Geotechnical Engineering* **108(3)**: 439–458.

Fan C-C and Long JH (2005) Assessment of existing methods for predicting soil response of laterally loaded piles in sand. *Computers and Geotechnics* **32(4)**: 274–289.

Gavin KG, Igoe JP and Doherty P (2011) Piles for offshore wind turbines: a state-of-the-art review. *Proceedings of the Institution of Civil Engineers*, *Geotechnical Engineering* **164(4)**: 245–256.

Hetenyi M (1946) *Beams on Elastic Foundation*. University of Michigan Press, Ann Arbor, MI.

Jardine RJ, Chow FC, Overy RF and Standing JR (2005) *ICP Design Methods for Driven Piles in Sands and Clays*. Thomas Telford, London.

Lam IPO (2009) *Diameter Effects on p–y Curves*. Deep Foundations Institute, Hawthorne, NJ.

Lam I and Martin G (1986) *Seismic Design of Highway Bridge Foundations Vol. II: Design Procedures and Guidelines*. Federal Highway Administration, Washington, DC, Report No. FHWA/RD-86/102.

Leblanc C, Houlsby GT and Byrne BW (2010) Response of stiff piles in sand to long-term cyclic lateral loading. *Géotechnique* **60(2)**: 79–90.

Lesny K and Wiemann J (2006) Finite-element-modelling of large diameter monopiles for offshore wind energy converters. *Proceedings of Geo Congress*, *Atlanta*, *GA*. ASCE, Reston, VA, pp. 1–6.

Lin SS and Liao JC (1999) Permanent strains of piles in sand due to cyclic lateral loads. *ASCE Journal of Geotechnical and Geoenvironmental Engineering* **125(9)**: 798–802.

Little RL and Briaud JL (1988) *Full Scale Lateral Load Tests on Six Single Piles in Sand*. Geotechnical Division, Texas A&M University, College Station, TX, miscellaneous paper GL-88-27.

Long JH and Vanneste G (1994) Effects of cyclic lateral loads on piles in sand. *ASCE Journal of Geotechnical and Geoenvironmental Engineering* **120(1)**: 225–244.

Matlock H (1970) Correlations for design of laterally loaded piles in soft clay. *Proceedings of the Offshore Technology Conference*, *Houston*, *TX*, pp. 577–594.

Mayne PW and Kulhawy FH (1982) K0–OCR relationships in soils. *ASCE Journal of Geotechnical Engineering Division* **108(6)**: 851–872.

Murchinson JM and O'Neill MW (1984) Evaluation of *p–y* relationships in cohesionless soil: analysis and design of pile foundations. *Proceedings of Symposium in Conjunction with the ASCE National Convention, San Francisco, CA*. ASCE Technical Council on Codes and Standards, New York, pp. 174–191.

Norris G (1986) Theoretically based BEF laterally loaded pile analysis. *Proceedings of the 3rd International Conference on Numerical Methods in Offshore Piling*, *Nantes*, Editions Technip, Paris, pp. 361–386.

Peck RB, Hanson WE and Thornburn TH (1953) *Foundation Engineering*. Wiley, New York.

Pender MJ (1993) Aseismic pile foundation design analysis. *Bulletin of the New Zealand National Society for Earthquake Engineering* **26(1)**: 49–160.

Poulos H and Hull T (1989) The role of analytical geomechanics in foundation engineering. In *Foundation Engineering: Current Principles and Practices*, vol. 2. ASCE, New York, pp. 1578–1606.

Reese LC and Matlock H (1956) Non-dimensional solutions for laterally loaded piles with soil modulus assumed proportional to depth. *Proceedings of the 8th Texas Conference on Soil Mechanics and Foundation Engineering*, *Austin*, *TX*, 1–41.

Reese LC, Cox WR and Koop FD (1974) Analysis of laterally loaded piles in sand. *Proceedings of the 6th Annual Offshore Technology Conference*, *Houston*, *TX*, 473–484.

Sørensen SPH, Brødbæk KT, Møller M, Augustesen AH and Ibsen LB (2009) Evaluation of the load–displacement relationships for large-diameter piles in sand. *Proceedings of the 12th International Conference on Civil, Structural and Environmental Engineering Computing* (Topping BHV, Costa Neves LF and Barros RC (eds)). Civil-Comp Press, Sterling, UK, Paper 244.

Terzaghi K (1955) Evaluation of coefficient of subgrade reaction. *Géotechnique* **5(4)**: 297–326.

Vesic AS (1961) Beam on elastic subgrade and Winkler's hypothesis. *Proceedings of the 5th International Conference on Soil Mechanics and Foundation Engineering*, *Paris*, pp. 845–850.